

High-temperature-resistant distributed Bragg reflector fiber laser written in Er/Yb co-doped fiber

Bai-Ou Guan^{1,2,*}, Yang Zhang^{1,2}, Hong-Jun Wang^{1,2}, Da Chen^{1,2}, and Hwa-Yaw Tam^{2,3}

¹ School of Physics & Optoelectronic Technology, Dalian University of Technology,
Dalian 116024, China

² PolyU-DUT Joint Research Center for Photonics, Dalian University of Technology,
Dalian 116024, China

³ Photonics Research Centre and Department of Electrical Engineering,
The Hong Kong Polytechnic University, Hong Kong, China

*Corresponding author: guanboo@yahoo.com

Abstract: We present a high-temperature-resistant distributed Bragg reflector fiber laser photowritten in Er/Yb codoped phosphosilicate fiber that is capable of long-term operation at 500 °C. Highly saturated Bragg gratings are directly inscribed into the Er/Yb fiber without hydrogen loading by using a 193 nm excimer laser and phase mask method. After annealing at elevated temperature, the remained gratings are strong enough for laser oscillation. The laser operates in robust single mode with output power more than 1 dBm and signal-to-noise ratio better than 70 dB over the entire temperature range from room temperature to 500 °C.

©2008 Optical Society of America

OCIS codes: (060.2370) Fiber optics sensors; (060.3510) Lasers, fiber; (060.3735) Fiber Bragg gratings; (120.6780) Temperature

References and links

1. D. J. Hill, P. J. Nash, D. A. Jackson, D. J. Webb, S. F. O'Neill, I. Bennion, and L. Zhang, "A fiber laser hydrophone array," in Proc. SPIE Conf. Fiber Optic Sensor Technology and Applications **3860**, (Boston, MA, 1999), 55–66.
2. S. W. Lovseth, J. T. Kringlebotn, E. Ronnekleiv, and K. Blotekjaer, "Fiber distributed-feedback lasers as acoustic sensors in air," Appl. Opt. **38**, 4821–4831 (1999).
3. R. I. Crickmore, M. J. Gunning, J. Stefanov, and J. P. Dakin, "Beat frequency measurement system for multiple dual polarization fiber DFB lasers," IEEE Sensor J. **3**, 115–120 (2003).
4. B. O. Guan, H. Y. Tam, S. T. Lau, and H. L. W. Chan, "Ultrasonic hydrophone based on distributed Bragg reflector fiber laser," IEEE Photo. Technol. Lett. **16**, 169–171 (2005).
5. A. D. Kersey, M. A. Davis, H. J. Patrick, M. LeBlanc, K. P. Koo, C. G. Askins, M. A. Putnam, and E. J. Friebele, "Fiber grating sensors," J. Lightwave Technol. **15**, 1442–1463 (1997).
6. J. L. Zysskind, V. Mizrahi, D. J. DiGiovanni, and J. W. Sulhoff, "Short single frequency erbium-doped fibre laser," Electron. Lett. **28**, 1385–1387 (1992).
7. J. T. Kringlebotn, J. L. Archambault, L. Reekie, J. E. Townsend, G. G. Vienne, and D. N. Payne, "Highly-efficient, low-noise grating-feedback Er:Yb codoped fibre laser," Electron. Lett. **30**, 972–973 (1994).
8. W. H. Loh, B. N. Samson, L. Dong, G. J. Cowle, and K. Hsu, "High performance single frequency fiber grating-based Erbium/Ytterbium-codoped fiber lasers," J. Lightwave Technol. **16**, 114–118 (1998).
9. C. Spiegelberg, J. Geng, Y. Hu, Y. Kaneda, S. Jiang, and N. Peyghambarian, "Low-noise narrow-linewidth fiber laser at 1550nm," J. Lightwave Technol. **22**, 57–62 (2004).
10. Y. Shen, Y. Qiu, B. Wu, W. Zhao, S. Chen, T. Sun, and K. T. V. Grattan, "Short cavity single frequency fiber laser for in-situ sensing applications over a wide temperature range," Opt. Express **15**, 363–370 (2007).
11. W. H. Loh, L. Dong, and J. E. Caplen, "Single-sided output Sn/Er/Yb distributed feedback fiber laser," Appl. Phys. Lett. **69**, 2151–2153 (1996).
12. Y. O. Barmenkov, D. Zalvidea, S. T. Peiro, J. L. Cruz, and M. V. Andres, "Effective length of short Fabry-Port cavity formed by uniform fiber Bragg gratings," Opt. Express **14**, 6394–6399 (2006).

1. Introduction

Fiber grating laser sensors have attracted considerable interests because they not only possess advantages of passive fiber grating sensors, such as compact size, inherent self-referencing capability, and multiplexing capability, but also offer higher signal-to-noise ratio. Depending on the operation principle, fiber grating laser sensors are classified into two categories, namely wavelength encoding sensor and polarimetric sensor. The former converts a measurand into a corresponding change in the operation wavelength of the laser [1, 2], which is similar to that of the fiber grating sensors. The polarimetric sensor requires the fiber grating laser to operate in two orthogonal polarization modes and converts a measurand into a corresponding change in the beat frequency generated by the two polarization modes of the laser [3, 4]. In this case, signal extraction is much simpler because the beat frequency is in the radio frequency (RF) domain, which eliminates expensive absolute wavelength measurement that is required in the passive fiber grating sensors [5]. Earlier reported fiber grating lasers were mainly fabricated in conventional Er-doped silica fiber [6]. As the lasers need to be no more than several cm in length to ensure robustly single mode operation, the output power was limited to the order of μW due to the low pump absorption. This problem was overcome by codoping the Er-doped fiber with Yb ions [7, 8]. The Yb ions exhibit strong absorption at 980 nm and then transfer their energy to the Er ions. This greatly increases the pump absorption, leading to increase in the laser efficiency and output power. Up to 200 mW at 1550 nm has been obtained with Er/Yb codoped phosphate glass fiber [9].

For sensor applications at high temperature environment, thermal resistance is a key issue. Recently Shen et al. demonstrated a scheme to construct distributed Bragg reflector (DBR) fiber laser by splicing a piece of Er-doped silica fiber to two high-temperature-sustainable Bragg gratings written in Bi-Ge codoped fiber [10]. The laser can survive at 400 °C, but the output power was limited to less than -15 dBm due to the low pump absorption of the Er-doped silica fiber and the intracavity splice loss. In this paper, we present a DBR fiber laser directly photowritten in commercial available Er/Yb codoped phosphosilicate fiber that is able to operate at 500 °C. The laser operates in robust single mode with output power more than 1 dBm and signal-to-noise ratio better than 70 dB over the entire temperature range from room temperature to 500 °C.

2. DBR fiber laser inscription

The active fiber used in the experiments was a commercial available Er/Yb codoped phosphosilicate fiber (DF1500Y, manufactured by Fibercore Ltd). The DBR lasers consisting of 11-mm-long high reflectivity grating, 9-mm-long output grating, and grating end-to-end separation of 5 mm, were fabricated by directly writing the grating pair into the Er/Yb fiber with an 193 nm excimer laser and an 25-mm-long phase mask. Thanks to the high efficiency at 193 nm associated with the two-photon excitation process, hydrogen-loading for enhancing the photosensitivity was not required. This not only simplifies the procedure for laser fabrication but also avoids the laser efficiency degradation arising from the hydrogen loading induced loss at pump wavelength [11]. Figure 1 shows the experimental setup for the DBR fiber laser inscription. The beam scanning technique was used, in which the phase mask and the fiber were fixed, while the laser beam scanned along the fiber. The two gratings were written with the same beam scanning speed so that they had the same ac and dc index change therefore the same center wavelength. The energy and repetition frequency of the 193 nm excimer laser were set to 5 mJ and 120 Hz, respectively. The beam scanning speed was set to 20 $\mu\text{m}/\text{sec}$.

We first wrote the high reflectivity grating. The grating transmission spectrum was monitored by using an Er-doped fiber amplified spontaneous emission (ASE) source and an optical spectrum analyzer (OSA). Figure 2 shows the growth of the grating during 193 nm UV inscription. From Fig. 2 it is clear that the grating is highly saturated. It is also seen from Fig. 2 that the rise in grating strength is accompanied by a blueshift of the grating wavelength. This is due to the heating effect induced by the UV irradiation and can be explained as follow.

The grating was inscribed by scanning a 2-mm-wide UV beam along the fiber at a constant speed. At the beginning, the grating length was about the same with the width of the UV beam, so the whole grating was heated by the beam, leading to a redshift of the grating wavelength. As the UV beam translates along the length of the fiber, the non UV-irradiate section of the grating cooled down and makes an increasing contribution to the transmission loss peak. Consequently the peak wavelength was determined by both the heated and unheated sections of the grating. The unheated section increased whereas the heated section was kept at 2 mm in length, therefore the grating wavelength shifted to shorter wavelength.

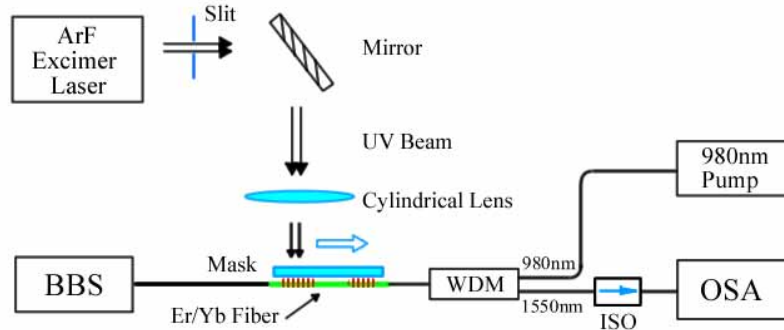


Fig. 1. Experimental setup for the DBR fiber laser inscription.

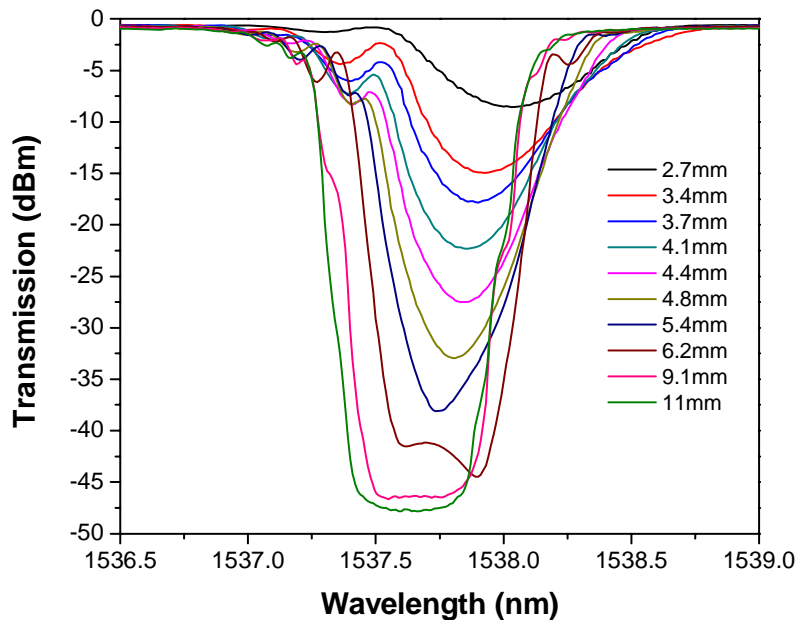


Fig. 2 Transmission spectra of the grating during UV inscription at different lengths.

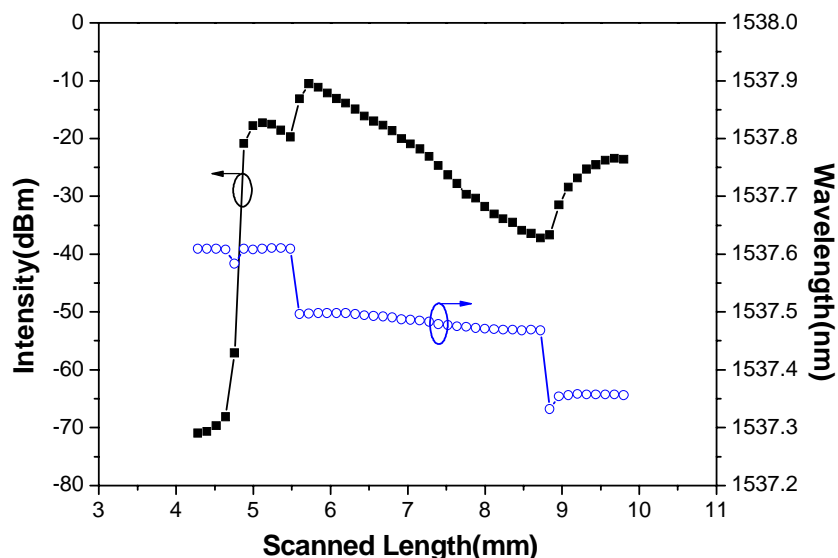


Fig. 3. Peak power and wavelength of the DBR laser versus the scanned length of the output grating.

We then wrote the output grating with the same beam scanning speed, while the ASE source was turned off and an 980 nm pump laser with 70 mW of output power was turned on so that the laser output could be monitored. Figure 3 illustrates the peak power and wavelength of the DBR fiber laser as functions of the scanned length. At the beginning, the grating reflectivity was too low and the gain could not compensate the high cavity loss, so the laser did not oscillate and only Fabry-Port interference fringe was observed. The fringe period decreased with time because the effective length of the laser cavity, which is the sum of the effective lengths of the two gratings and grating separation [12], increased with the grating length. The laser started to oscillate when the output grating length reach to around 4.7 mm, then the laser output power increased sharply. After it reached a maximum value, the output power decreased slowly. In this process mode hopping occurred twice, each time followed by an increase in output power. It can be seen from Fig. 3 that the laser always hops down to the adjacent lower wavelength mode. This can be explained by the blueshift of the grating wavelength during the UV beam scanning as shown in Fig. 2. The grating blueshift changes the wavelength of the minimum loss (i.e. maximum net gain) to lower wavelength, which causes the laser to mode hop to the next mode down in wavelength.

Because the gratings were highly saturated, it is expected that, after subjected to a significant decay at elevated temperature, the remained grating will be strong enough for laser oscillation.

3. Annealing and thermal response

The DBR laser was then put into a tube oven for annealing and thermal response test. The laser was heated up to 600 °C, while the laser output spectrum was monitored. Figure 4 shows the laser spectra evolution as temperature increases. The output grating was highly saturated and its reflectivity was very high and so very small optical output was emit by the laser. The laser output power increased with the decay of the reflectivity of the output grating. A maximum output power (peak power) of 7.8 dBm was recorded at 555 °C. Subsequently, the laser output power decreased following further decay of the gratings. The output power remained at 6 dBm when the temperature reached 600 °C. It took about 15 minutes for the oven to rise from room temperature to 600 °C. In the process, mode hopping occurred three times. Similar to that occurred during the laser inscription, the laser always hop to the adjacent lower wavelength mode. This is the result of the blueshift of the grating wavelength, which is

induced by the decrease of the average index arising from the drop of the index modulation depth. After staying at 600 °C for a couple of minutes, the oven temperature was set to 500 °C. Figure 5 shows the thermal stability of the DBR laser at 500 °C. No decrease in laser power was observed after 1 hour of annealing.

The oven was then switched off and the temperature dropped from 500°C to room temperature, while the laser output spectra was recorded with the OSA. Figure 6 illustrates the peak power and wavelength of the DBR fiber laser as function of temperature. Figure 7 shows the laser spectra at different temperatures. The laser operated in robust single mode with output power over 1 dBm and signal-to-noise ratio over 70 dB in the entire temperature range.

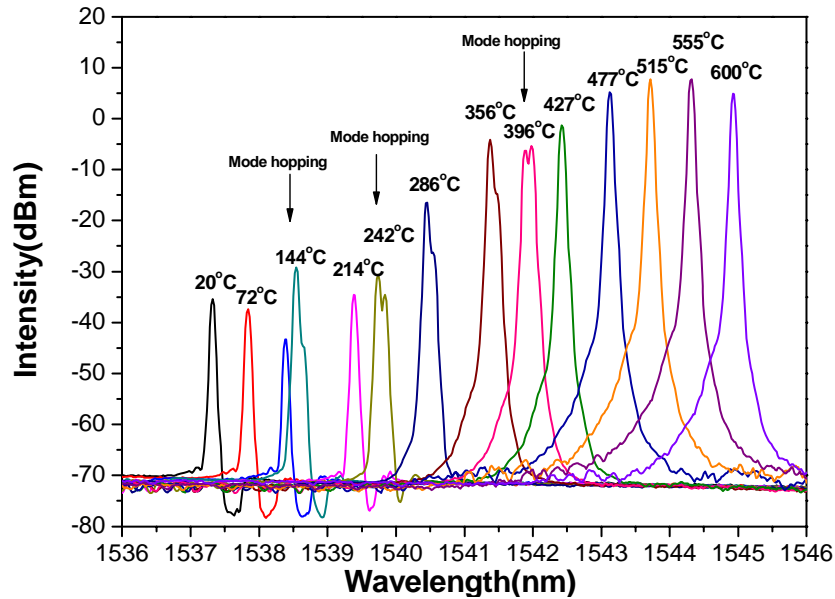


Fig. 4. Evolution of the laser spectra during the annealing process in which the temperature increased from room temperature to 600 °C.

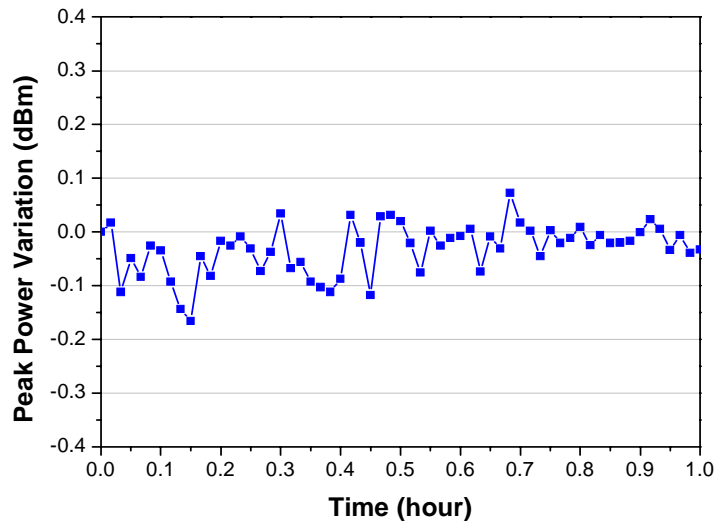


Fig. 5. Stability of the DBR laser output peak power at 500°C

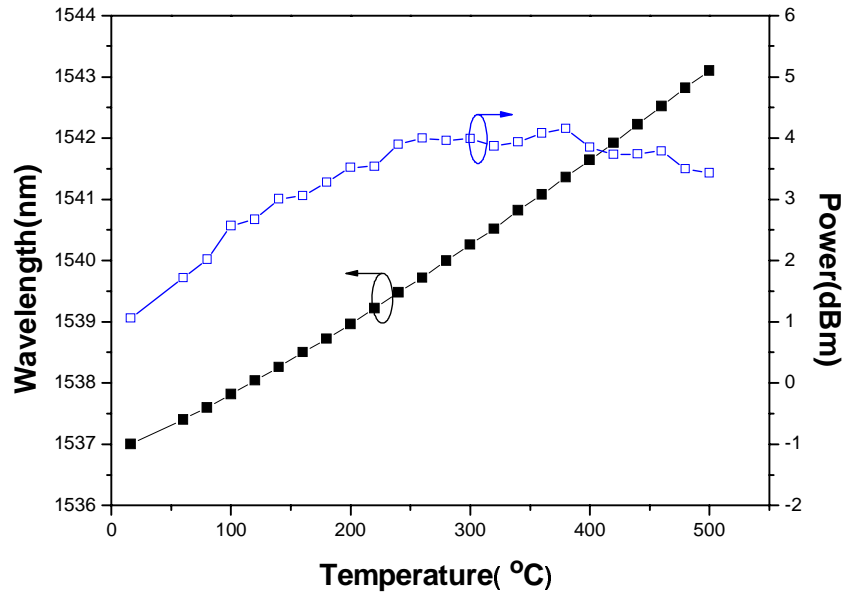


Fig. 6. The peak power and wavelength of the DBR laser versus temperature.

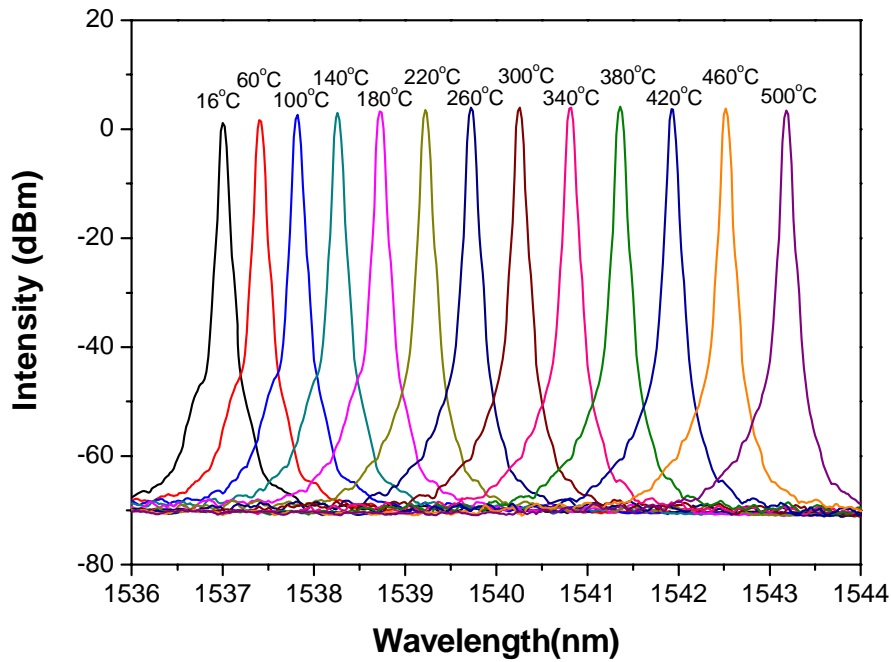


Fig. 7. The laser spectra at different temperature.

It is worth noting that, after annealing, the laser output power is much higher than the maximum power obtained during the DBR laser fabrication. We repeated the experiments by writing some DBR lasers and then heating them at the same condition. For all lasers, the maximum output during UV inscription was less than -9 dBm, whereas the output power after

annealing increased to several dBm. A possible reason is that the annealing process greatly increased the effective length of the laser cavity. Because both gratings were highly saturated, almost 99% of light was reflected by the 2 mm sections at the front of the grating, so although the physical length of the cavity was 25 mm, the effective length that contributes to laser operation was only a little longer than the separation between gratings, 5 mm. After annealing, the gratings became moderately modulated and the light was reflected distributely along the length of the grating. This makes the effective cavity length significantly longer, leading to an increase in laser output.

4. Conclusion

We have demonstrated a high-temperature-resistant DBR fiber laser in Er/Yb co-doped phosphosilicate fiber that is capable of long-term operation at 500 °C. The DBR laser was fabricated by directly photowriting a pair of highly saturated Bragg gratings into the Er/Yb fiber with a 193 nm eximer laser and phase mask method. After subjected to a significant decay at high temperature, the remained grating was strong enough for laser oscillation. The laser operated in robust single mode with output power more than 1 dBm and signal-to-noise ratio better than 70 dB over the entire temperature range from room temperature to 500 °C.

Acknowledgments

This work was supported by Program for New Century Excellent Talents in University (NCET-06-0271) and National Natural Science Foundation of China (Project No.60736039).